Nonlinear lattices generated from harmonic lattices with geometric constraints

S. Takeno,[1] S. V. Dmitriev,[2,3] P. G. Kevrekidis,[4] and A. R. Bishop[5]
[1]*Graduate School, Nagasaki Institute of Applied Science, Nagasaki 851-0193, Japan*
[2]*Institute of Industrial Science, University of Tokyo, 4-6-1 Komaba, Meguro-ku, Tokyo 153-8505, Japan*
[3]*National Institute of Materials Science, 1-2-1 Sengen, Tsukuba, Ibaraki 305-0047, Japan*
[4]*Department of Mathematics and Statistics, University of Massachusetts, Lederle Graduate Research Tower, Amherst, Massachusetts 01003-4515, USA*
[5]*Center for Nonlinear Studies and Theoretical Division, Los Alamos National Laboratory, Los Alamos, New Mexico 87545, USA*
(Received 11 August 2004; published 20 January 2005)

Geometrical constraints imposed on higher-dimensional harmonic lattices generally lead to nonlinear dynamical lattice models. Helical lattices obtained by such a procedure are shown to be described by sine- plus linear-lattice equations. The interplay between sinusoidal and quadratic potential terms in such models is shown to yield localized nonlinear modes identified as intrinsic resonant modes.

DOI: 10.1103/PhysRevB.71.014304 PACS number(s): 63.20.Pw, 05.45.Yv, 63.10.+a

I. INTRODUCTION

Recent developments in the physics of intrinsic localized modes (ILM)[1,2] have shown that the ILMs are not only conceptually important in theoretical and mathematical physics as ubiquitous fundamental modes in nonlinear, discrete physical systems,[3] but also possess innovative potential applications in fundamental science and technology in addition to their experimental observation.[4–6] Areas of such applications cover coupled Josephson junctions, photonic crystals, optical lattices in Bose-Einstein condensates, all-optical logic and switching devices, targeted breaking of chemical bonds, and so on.[7]

Very recently, the interplay between nonlinear dynamics and geometry has attracted particular attention in ILM problems.[8] Historically, such an observation was made when formulating model Hamiltonians for the dynamics of bases in DNA to take care of helical structure.[9,10] The latter problem gave rise to the intuitive introduction of the so-called sine-lattice (SL) model[11] in which intersite interactions along a given strand are taken to be sinusoidal rather than the conventional quadratic ones. The SL model later turned out to yield a different type of ILM, referred to as an intrinsic rotating mode (IRM), also termed a roto-breather.[12] An example of transition from oscillation to such rotation modes in simulations of molecular crystals can be found in Ref. 13. Another example of this type is given by curved or bent chains[14] and long-range interactions on a fixed curved substrate.[15]

Geometric constraints naturally appear in crystalline bodies consisting of relatively rigid atomic clusters. An important example of this class of materials are the polymorphs of silica (SiO_2), where the structural units (i.e., SiO_4 tetrahedra) are corner-linked by oxygen atoms, and the energy cost of deformation of the tetrahedra is much greater than the cost of their mutual rotations. Atoms in the almost rigid clusters move as if they were subjected to a geometrical constraint. To describe the position of a finite-size molecular cluster, one has to introduce not only translational but also rotational degrees of freedom. It has been demonstrated that the rotational degrees of freedom can be responsible for the incommensurate phase in quartz,[16–18] negative Poisson ratio of cristobalite and quartz,[19–22] and negative thermal expansion of β quartz.[23] Similar effects can be observed in other materials with microscopic rotations, such as perovskites (e.g., $SrTiO_3$) containing corner-linked TiO_6 octahedra, the KH_2PO_4 (KDP) family of crystals with comparatively rigid PO_4 tetrahedra, among others.

Motivated by these investigations, we proposed in a previous paper a mechanical model in which a set of masses on a linear chain are rearranged to slide on fixed rings.[24] Such a model was shown to contain rich nonlinear dynamics, exhibiting various types of nonlinear modes ranging from kinks to IRMs. The method employed there amounts to applying a specific geometrical constraint to a purely harmonic lattice, leading eventually to equations having the form of an extended version of the SL equations.

It is our purpose here to propose a method for studying the above-mentioned interplay between nonlinearity and geometry in a more general and transparent (than our earlier work) way. The basic point of our method is to take three-dimensional (3D) harmonic lattices as a starting point on which geometrical constraints are imposed. Since linear systems constitute a basis for studying physics and mathematics, in general, we expect the present method will give much more insight into the problem. The work is composed of two parts: the first presents a general scheme of geometrical constraints, while the second complements it with a detailed study of the ILMs in sine plus linear lattices resulting from the helical constraints that we impose on the original 3D harmonic lattice.

This paper is organized as follows. In Sec. II, we present a simple 3D harmonic-lattice model and consider a general scheme of the geometrical constraint applied to it. In Sec. III, we introduce the helical constraints as an application of the general method to arrive at helical lattices described by sine-linear-lattice (SLL) equations interpolating between SL and linear lattice. Section IV is devoted to the study of some properties of the SLL equations. Generalization of the SLL model is made in Sec. V to include the effect of an on-site

potential, giving rise to the ILMs. Section VI is devoted to concluding remarks.

II. LINEAR LATTICE MODEL AND A GEOMETRIC CONSTRAINT

We consider a three-dimensional lattice governed by the Lagrangian L

$$\begin{aligned} L &= T - V \\ &\equiv \sum_n \frac{m_n}{2}(\dot{x}_n^2 + \dot{y}_n^2 + \dot{z}_n^2) - \frac{K}{2}\sum_n [(x_{n+1} - x_n)^2 \\ &\quad + (y_{n+1} - y_n)^2 + (z_{n+1} - z_n)^2], \end{aligned} \tag{1}$$

where T and U are the kinetic energy and the potential energy of the system, respectively. The quantities x_n, y_n, and z_n are the dynamical variables associated with the nth atom of atomic mass m_n. Then, the Euler-Lagrange equations assume the form

$$\begin{aligned} m_n \frac{d^2 x_n}{dt^2} &= K(x_{n+1} + x_{n-1} - 2x_n), \\ m_n \frac{d^2 y_n}{dt^2} &= K(y_{n+1} + y_{n-1} - 2y_n), \\ m_n \frac{d^2 z_n}{dt^2} &= K(z_{n+1} + z_{n-1} - 2z_n). \end{aligned} \tag{2}$$

Physically, Eqs. (2) are equations of motion for harmonic-lattice vibrations of a simplified version of a simple cubic lattice, in which x_n, y_n, and z_n represent the x, y, and z components of the displacement vector $\vec{r}_n$ of the nth atom from its equilibrium position.

Suppose now that there exists a single variable s such that

$$x_n = f(s_n), \quad y_n = g(s_n), \quad z_n = h(s_n), \tag{3}$$

where $f(s)$, $g(s)$, and $h(s)$ are functions of s. The Lagrangian of the system is then written as

$$\begin{aligned} L &= \frac{1}{2}\sum_n m_n[f'(s_n)^2 + g'(s_n)^2 + h'(s_n)^2]\dot{s}^2 \\ &\quad - \frac{K}{2}\sum_n \{[f(s_{n+1}) - f(s_n)]^2 \\ &\quad + [g(s_{n+1}) - g(s_n)]^2 + [h(s_{n+1}) - h(s_n)]^2\}. \end{aligned} \tag{4}$$

Then, the Euler-Lagrange equations takes the form

$$\begin{aligned} &m_n[f'(s_n)^2 + g'(s_n)^2 + h'(s_n)^2]\ddot{s}_n \\ &\quad + \frac{m_n}{2}\left\{\frac{d}{ds}[f'(s_n)^2 + g'(s_n)^2 + h'(s_n)^2]\right\}\dot{s}_n^2 \\ &\quad = K[f(s_{n+1}) + f(s_{n-1}) - 2f(s_n)]f'(s_n) \\ &\quad\quad + K[g(s_{n+1}) + g(s_{n-1}) - 2g(s_n)]g'(s_n) \\ &\quad\quad + K[h(s_{n+1}) + h(s_{n-1}) - 2h(s_n)]h'(s_n), \end{aligned} \tag{5}$$

where $A'(s) \equiv (d/ds)A(s)$ with $A = f, g, h$. It can, hence, be seen from Eqs. (4) and (5) that the geometric constraint of Eqs. (3) transforms the original linear lattice equations into nonlinear ones. Thus, depending on the choice of f, g, and h, we can obtain various nonlinear equations from the linear-lattice model through the one-parameter geometric constraint. Equations (3) can be generalized to the case in which, e.g., the quantities x_n and y_n are parametrized by two variables, (s_{1n}, s_{2n}).

III. HELICAL CONSTRAINT AND THE SINE-LINEAR LATTICE

We illustrate the above method by considering situations in which the constraint functions f, g, and h are of the form

$$\begin{aligned} f(s_n) &= a_n \cos(cs_n) \equiv a_n \cos(\theta_n), \\ g(s_n) &= a_n \sin(cs_n) \equiv a_n \sin(\theta_n), \\ z_n &= v_n s_n \equiv b_n \theta_n, \end{aligned} \tag{6}$$

where c, a_n, and v_n are constants depending on the site index n and $b_n = v_n/c$. Inserting Eqs. (6) into Eq. (4), we obtain the Lagrangian of the system in the form

$$\begin{aligned} L &= T - U \\ &= \sum_n \left[\frac{m_n}{2}(a_n^2 + b_n^2)\dot{\theta}_n^2\right] - \sum_n \frac{K}{2}[a_{n+1}^2 + a_n^2 - 2a_{n+1}a_n \\ &\quad \times \cos(\theta_{n+1} - \theta_n) + (b_{n+1}\theta_{n+1} - b_n\theta_n)^2]. \end{aligned} \tag{7}$$

Then, the Euler-Lagrange equations are given by

$$\begin{aligned} \ddot{\theta}_n &= C_n[a_{n+1}a_n \sin(\theta_{n+1} - \theta_n) - a_n a_{n-1} \sin(\theta_n - \theta_{n-1})] \\ &\quad + C_n[b_{n+1}b_n\theta_{n+1} + b_n b_{n-1}\theta_{n-1} - 2b_n^2\theta_n], \end{aligned} \tag{8}$$

where

$$C_n = \frac{K}{m_n(a_n^2 + b_n^2)}. \tag{9}$$

Equation (8) interpolates between a generalized version of the linear lattice

$$\ddot{\theta}_n = C_n[b_{n+1}b_n\theta_{n+1} + b_n b_{n-1}\theta_{n-1} - 2b_n^2\theta_n] \tag{10}$$

and that of the sine-lattice equation[10,11]

$$\ddot{\theta}_n = C_n[a_{n+1}a_n \sin(\theta_{n+1} - \theta_n) - a_n a_{n-1} \sin(\theta_n - \theta_{n-1})], \tag{11}$$

where the coefficients on the right-hand side are all site dependent. Equation (8) is referred to as a sine-linear-lattice (SLL) equation.

IV. A PERFECT HELICAL LATTICE

Here we restrict ourselves to the simplest of situations in which all the coefficients are site independent. Then, dropping the subscript n attached to the coefficients in Eq. (8) leads to

$$\ddot{\theta}_n = J[\sin(\theta_{n+1} - \theta_n) - \sin(\theta_n - \theta_{n-1}) + \epsilon(\theta_{n+1} + \theta_{n-1} - 2\theta_n)], \tag{12}$$

where

$$J = Ca^2, \quad \epsilon = b^2/a^2. \tag{13}$$

The nonintegrable equation (12) can be considered as relevant to helical lattices in which the helicity is determined by the factor ϵ. Alternatively, Eq. (12) may be considered as a modified version of the discrete sine-Gordon equation[25] in which the conventional on-site term $\sin(\theta_n)$ is replaced by the first term on the right-hand side of Eq. (12).

A. Steady-state structures

Equation (12) can be rewritten in the form

$$\ddot{\theta}_n = J(D_n - D_{n-1}),$$

$$D_n = \sin(\delta_n) + \epsilon\delta_n, \quad \delta_n = \theta_{n+1} - \theta_n. \tag{14}$$

Equilibrium solutions to Eq. (14) can be found from $D_n = D_{n-1}$, which is particularly satisfied when

$$D_n = 0 \tag{15}$$

for all n. Stable equilibria are subjected to an additional condition, $D_n'(\delta_n) = \cos(\delta_n) + \epsilon > 0$.

To study the physical properties of Eq. (12), which represents the competition between the linearity and the helicity, let us consider the potential function $V(\delta_n)$ associated with $D_n(\delta_n)$,

$$V(\delta_n) = 1 - \cos(\delta_n) + \epsilon\frac{\delta_n^2}{2}, \quad \epsilon > 0. \tag{16}$$

We pay particular attention to its minimum points. For sufficiently large ϵ (weak helicity), the potential V has only one minimum at $\delta_n = 0$ and the only stable state of the SLL is the ground state, $\theta_n = \text{const}$. However, with a decrease of ϵ, new minima appear in the potential $V(\delta_n)$, the lth minimum appearing at

$$\epsilon_l \approx (4l-1)\frac{\pi}{2} - \sqrt{(4l-1)^2\frac{\pi^2}{4} - 2}, \quad l > 0. \tag{17}$$

For example, $\epsilon_1 \approx 0.2172$, $\epsilon_2 \approx 0.091\,33$, and $\epsilon_3 \approx 0.057\,97$. The potential $V(\delta_n)$ is shown in Fig. 1 for these values of ϵ and also for a larger magnitude, $\epsilon = 0.4$, when there is only one minimum. In the limiting case $\epsilon \to 0$, the SLL Eq. (12) degenerates to the SL equation with energetically indistinguishable minima situated at $\delta_n = 2\pi l$.

As the number of minima on the potential $V(\delta_n)$ increases, the variety of the stable structures of the SLL Eq. (12) also increases. For $\epsilon_{l+1} < \epsilon < \epsilon_l$, δ_n can obtain $2(l-1)$ values (positive or negative) in addition to $\delta_n = 0$, which is allowed for any ϵ.

For the particular class of equilibrium solutions expressed by Eq. (15), configuration of the nth bond, $\delta_n = \theta_{n+1} - \theta_n$, is not affected by the adjacent bonds, and one can easily create various compactonlike localized defects. For example, for $\epsilon = 0.2$, $V(\delta_n)$ has minima at $\delta_n = 0$ and $\delta_n = \pm 4.9063$. In Fig. 2 we show several stable configurations of SLL at $\epsilon = 0.2$ and $J = 1$. Shown are (a) a kink-type structure, (b) a point defect in a ground-state structure, (c) a zigzag periodic structure, and (d) a point defect in the zigzag structure. The defects in periodic structures presented in Fig. 2 can be regarded as discrete compactons[26] because they are sharply localized and do not have exponential tails.

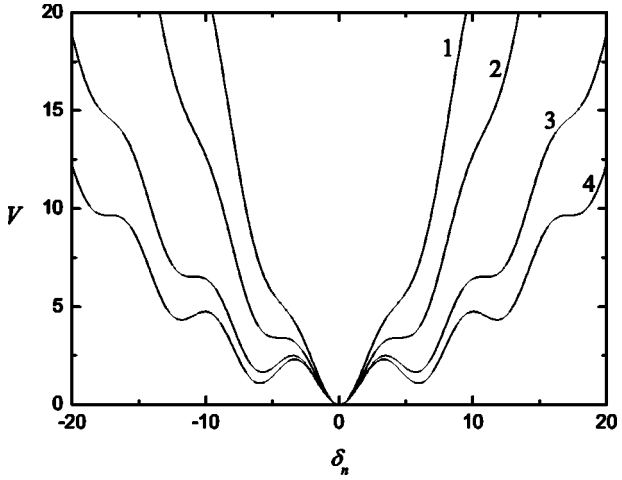

FIG. 1. The potential $V(\delta_n)$ of Eq. (16) is shown as a function of δ_n for different magnitudes of ϵ. Curves 1–4 correspond to $\epsilon = 0.4$, $\epsilon_1 \approx 0.2172$, $\epsilon_2 \approx 0.091\,33$, and $\epsilon_3 \approx 0.057\,97$. The magnitudes ϵ_l, at which lth minimum of the potential function appears, are given by Eq. (17).

B. Perturbation-induced dynamical structures

A vibration mode can be excited on the defect in zigzag structure presented in Fig. 2(d). The mode is (practically) localized on three particles; it is presented in Fig. 3. The existence of this mode can be easily understood. The zeroth particle in Fig. 2(d) oscillates with a frequency close to the upper edge of the ground state spectrum, which, however, is

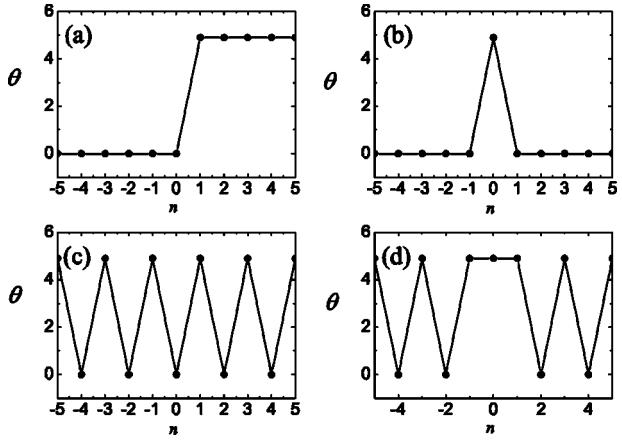

FIG. 2. Examples of stable equilibrium structures in SLL with $J = 1$, $\epsilon = 0.2$. (a) Kinklike structure, (b) point defect in the ground-state structure, (c) zigzag structure, and (d) point defect in the zigzag structure.

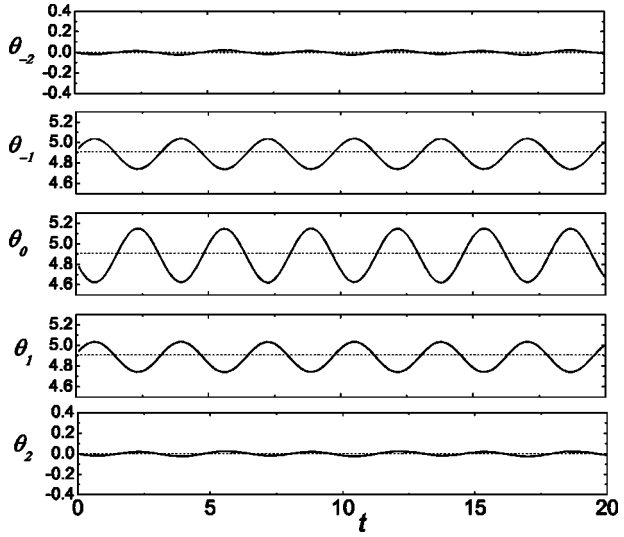

FIG. 3. Vibration mode excited for zigzag metastable structure with a defect present in Fig. 2(d). The mode is localized on (practically only) three particles. $J=1$ and $\epsilon=0.2$.

outside of the frequency band of the zigzag structure.

Due to translational invariance, the SLL model of Eq. (12) admits solutions with $\theta_n=\varphi$ for arbitrary $\varphi=$const. Domain walls separating two domains with $\varphi_1\neq\varphi_2$ can also be formed. Here we consider the case when the difference $|\varphi_1-\varphi_2|$ is not equal to the distance between the minima of the potential $V(\delta_n)$ Eq. (16) and that can give rise to moving kinks. There are many possibilities to initiate such moving kinklike structures; one is presented in Fig. 4 for $J=1$ and $\epsilon=0.2$. Here the kinks were initiated by applying initial conditions $\theta_0(0)=0$, $\dot{\theta}_0(0)=3$, with zero initial conditions for all other particles. The height of the kinks is $|\varphi_1-\varphi_2|\approx 0.9\pi$, and it increases by increasing the initial velocity of the zeroth particle. Here we use periodic boundary conditions to demonstrate that the kinks survive collisions and, hence, are relatively robust objects.

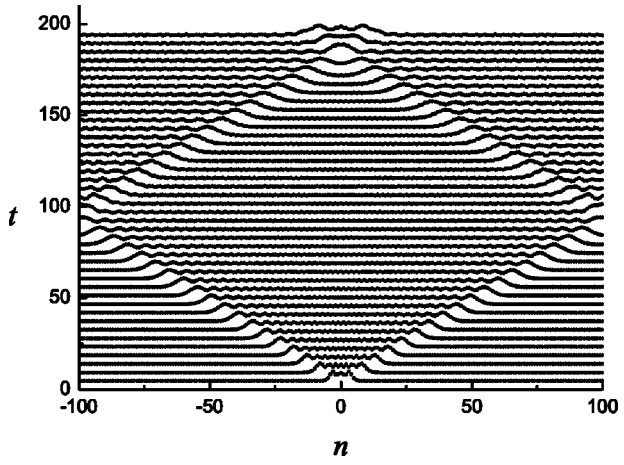

FIG. 4. Moving kinks initiated by the initial condition $\theta_0(0)=0$, $\dot{\theta}_0(0)=3$, and zero initial conditions for all other particles, presented by the set of plots θ vs n for different times. The height of the kinks is $|\varphi_1-\varphi_2|\approx 0.9\pi$, and it increases with increase in initial velocity of zeroth particle. Periodic boundary conditions are used here to demonstrate the kinks' robustness against collisions. $J=1$, and $\epsilon=0.2$.

C. An approximate analytical solution: Nonlinear resonant modes (NRM)

Let us consider situation in which an atom located at the site 0 makes a large excursion around one of the minimum points α of the potential, while the others only perform small amplitude oscillatory motion. This means that

$$|\theta_0| \gg |\theta_n| \text{ for } |n| \geq 1. \tag{18}$$

As we expect a highly localized solution, we preserve the full nonlinearity of the equations for the central site only, while the other equations are linearized around the equilibrium position. Such a procedure leads to

$$\ddot{\theta}_0 = J\{-2[\sin(\theta_0)+\epsilon\theta_0]+[\cos(\theta_0)+\epsilon](\theta_1+\theta_{-1})\}, \tag{19}$$

$$\ddot{\theta}_{\pm 1} = J\{-[\cos(\theta_0)+1+2\epsilon]\theta_{\pm 1}+(1+\epsilon)\theta_{\pm 2}+\sin(\theta_0)+\epsilon\theta_0], \tag{20}$$

$$\ddot{\theta}_n = J(1+\epsilon)(\theta_{n+1}+\theta_{n-1}-2\theta_n), \quad \text{for } |n|\geq 2. \tag{21}$$

We now seek solutions to this set of equations in the form

$$\theta_0 = \alpha + u_0, \quad \text{with } \sin(\alpha)+\epsilon\alpha = 0,$$

$$\theta_n \equiv u_n, \quad \text{for } |n|\geq 1. \tag{22}$$

When, in Eq. (22) $\alpha=0$, all particles oscillate near one well of the potential $V(\delta_n)$, while for $\alpha\neq 0$ the zeroth particle oscillates in a different well.

Inserting Eq. (22) into Eqs. (19)–(21) and retaining solely terms linear with respect to u_0 and $u_n(n\neq 0)$, we arrive at a set of equations that are of the same form as those appearing in one-impurity problems in harmonic-lattice vibrations. Thus, setting

$$u_n = v_n \exp(-i\omega t), \tag{23}$$

where v_n is time independent and ω is a constant, we reduce the above set of equations to the form

$$(L^{(0)}-\omega^2)v_n = L' v_n,$$

$$\text{with } L^{(0)}v_n = J(1+\epsilon)(2v_n - v_{n+1} - v_{n-1}), \tag{24}$$

with

$$L'v_0 = J[1-\cos(\alpha)](2v_0 - v_1 - v_{-1}),$$

$$L'v_{\pm 1} = J[1-\cos(\alpha)](v_{\pm 1} - v_0),$$

$$L'v_n = 0 \text{ for } n \neq 0, \pm 1. \tag{25}$$

From the above equations, the ILMs we are seeking are presumed to exist within the frequency band $\omega(k)^2$

$=2J(1+\epsilon)[1-\cos(k)]$ of the perfect harmonic lattice characterized by wavenumber k. Such a nonlinear localized in-band modes are referred to as (intrinsic) nonlinear resonant modes (NRM). Then, Eqs. (24) and (25) can be handled by introducing lattice Green's functions

$$g(n) \equiv g(n,\omega^2) = \frac{1}{N}\sum_k \frac{\exp(ikn)}{2J(1+\epsilon)[1-\cos(k)] - \omega^2 - i\gamma},$$

$$\gamma \to 0_+. \tag{26}$$

Analytical expressions for the lattice Green's functions $g(n)$ can be obtained by replacing the sum with respect to k by an integral over the first Brillouin zone as follows:

$$g(n) = \frac{1}{2J(1+\epsilon)}\frac{1}{\pi}\int_0^\pi \frac{\cos(nx)dx}{y-\cos(x)-i\gamma}$$

$$= \frac{i^{n+1}}{2J(1+\epsilon)}[C_n(y) - iS_n(y)], \tag{27}$$

where

$$C_n(y) = \int_0^\infty \cos(yt)J_n(t)dt,$$

$$S_n(y) = \int_0^\infty \sin(yt)J_n(t)dt,$$

$$\text{with } y = 1 - \frac{\omega^2}{2J(1+\epsilon)}, \tag{28}$$

in which $J_n(t)$ is the Bessel function of the nth order. We note that the quantity

$$C_0(y) = \frac{1}{\sqrt{1-y^2}},$$

$$\text{with } S_0(y) = 0 \text{ for } 0 < y < 1, \tag{29}$$

represents the density of states of the band. In terms of the $g(n)$'s so obtained, Eqs. (24) and (25) are rewritten as

$$u_n = J[1-\cos(k)][g(n)(2v_0 - v_1 - v_{-1}) + g(n-1)(v_1 - v_0) + g(n+1)(v_{-1} - v_0)]. \tag{30}$$

We pay particular attention to an s-like mode having the symmetry property

$$v_1 = v_{-1} \tag{31}$$

and use the identity relation

$$J(1+\epsilon)[2g(n) - g(n+1) - g(n-1)] - \omega^2 g(n) = \Delta_n \tag{32}$$

to obtain

$$v_n = \lambda[\omega^2 g(n) + \Delta_n](v_0 - v_1), \tag{33}$$

where

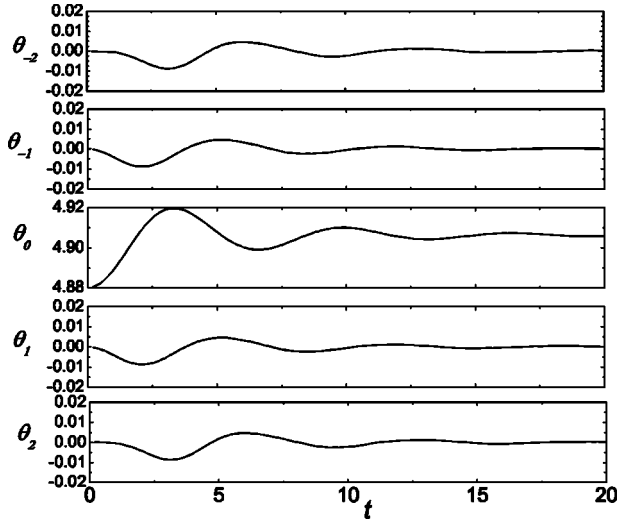

FIG. 5. An attempt to excite a NRM in a SLL lattice Eqs. (12) by means of initial conditions $\theta_0(0)=4.88$, $\dot{\theta}_0(0)=0$, with zero initial conditions for all other particles. $J=1$ and $\epsilon=0.2$. The zeroth particle oscillates near the minimum of $V(\delta_n)$ situated at $\delta_n \approx 4.9063$, while other particles oscillate near the minimum at $\delta_n = 0$. Due to the rather strong interaction with the lattice, the energy of excitation is "dissipated" to the lattice after only a few oscillations.

$$\lambda = \frac{1-\cos(\alpha)}{1+\epsilon} \tag{34}$$

and Δ_n are Kronecker's delta.

In terms of the dimensionless frequency $\xi = \omega^2/2J(1+\epsilon)$, an equation giving the eigenfrequency of the NRM is obtained from Eqs. (27), (29), and (33) as follows:

$$1 - \lambda - \lambda\xi - i\lambda\xi^2 C_0(y) = 0. \tag{35}$$

The dimensionless squared eigenfrequency ξ is therefore obtained as

$$\xi = \frac{1-\lambda}{\lambda} + i\xi_0\sqrt{\frac{\xi_0}{2-\xi_0}}. \tag{36}$$

The localization of the NRM is given by the equation

$$v_n = \lambda\omega^2 g(n)(v_0 - v_1), \quad n \neq 0. \tag{37}$$

As mentioned before, here the localized mode around the local minimum point of the potential function is of resonant type, the eigenfrequency that appears close to bottom of the frequency band $\omega(k)^2 = 2J(1+\epsilon)[1-\cos(k)]$. Apart from the factor α, which is the position of the local minimum, the localization properties of the NRM are essentially different from those of the ILM in that it exhibits oscillatory slow decay, contrary to what is the case for the ILM. This point will be examined in detail below.

We have attempted to excite NRMs in SLL of Eqs. (12). Such a numerical calculation is presented in Fig. 5. Here we set $J=1$, $\epsilon=0.2$, and for the initial conditions, $\theta_0(0)=4.88$ and $\dot{\theta}_0(0)=0$, with zero initial conditions for all other par-

ticles. For this choice of ϵ, the potential $V(\delta_n)$ has minima at $\delta_n=0$ and $\delta_n \approx \pm 4.9063$. One can see that the zeroth particle oscillates near the minimum of $V(\delta_n)$ situated at $\delta_n \approx 4.9063$, while the remaining particles oscillate near the minimum at $\delta_n=0$. Due to the rather strong interaction with the linear excitations of the lattice, the energy of the NRM is rapidly imparted to the lattice (after a few oscillations). The lifetime of the excitation does not increase much, either by changing the initial deviation of the zeroth particle from the potential minimum or by changing ε.

V. INCLUSION OF THE ON-SITE POTENTIAL

A. Derivation of the model

It is of interest to see what happens if we include on-site potentials in our original lattice. This is done by generalizing Eq. (1) in the form

$$L = \sum_n \frac{m_n}{2}(\dot{x}_n^2 + \dot{y}_n^2 + \dot{z}_n^2) - \frac{K}{2}\sum_n \Bigg[(x_{n+1} - x_n)^2 + (y_{n+1} - y_n)^2 + (z_{n+1} - z_n)^2 + \frac{\kappa_1}{2}x_n^2 + \frac{\kappa_2}{2}y_n^2 \Bigg], \quad (38)$$

where κ_1 and κ_2 are constants. Applying the helical constraint, Eq. (6) leads to

$$\begin{aligned} L &= K - U \\ &= \sum_n \left[\frac{m_n}{2}(a_n^2 + b_n^2)\dot{\theta}_n^2 \right] \\ &\quad - \sum_n \frac{K}{2}\Bigg[a_{n+1}^2 + a_n^2 - 2a_{n+1}a_n \cos(\theta_{n+1} - \theta_n) \\ &\quad + (b_{n+1}\theta_{n+1} - b_n\theta_n)^2 + \frac{a_n^2(\kappa_2 - \kappa_1)}{4}\cos[1 - \cos(2\theta_n)] \Bigg]. \end{aligned} \quad (39)$$

It is seen that such a procedure adds a sine-Gordon-type on-site potential $1-\cos(2\theta_n)$ to the Lagrangian. The equations of motion for θ_n then assume the form

$$\begin{aligned} \ddot{\theta}_n &= L_n[a_{n+1}a_n \sin(\theta_{n+1} - \theta_n) - a_n a_{n-1}\sin(\theta_n - \theta_{n-1}) \\ &\quad - \lambda a_n^2 \sin(2\theta_n)] + L_n[b_{n+1}b_n\theta_{n+1} + b_n b_{n-1}\theta_{n-1} \\ &\quad - (b_{n+1}b_n + b_n b_{n-1})\theta_n], \end{aligned} \quad (40)$$

where $\lambda=(\kappa_2-\kappa_1)/2$. When all the coefficients are site independent, the above equations reduce to

$$\begin{aligned} \ddot{\theta}_n &= J[\sin(\theta_{n+1} - \theta_n) - \sin(\theta_n - \theta_{n-1}) - \lambda \sin(2\theta_n) \\ &\quad + \epsilon(\theta_{n+1} + \theta_{n-1} - 2\theta_n)]. \end{aligned} \quad (41)$$

The presence of the on-site potential here can be speculated to induce the existence of localized modes with longer lifetime than that of the case of Eq. (12). In the following, we demonstrate the existence of ILMs in the model of Eq. (41).

B. Intrinsic localized modes

The linear spectrum of the SLL with the on-site potential, Eq. (41), is given by

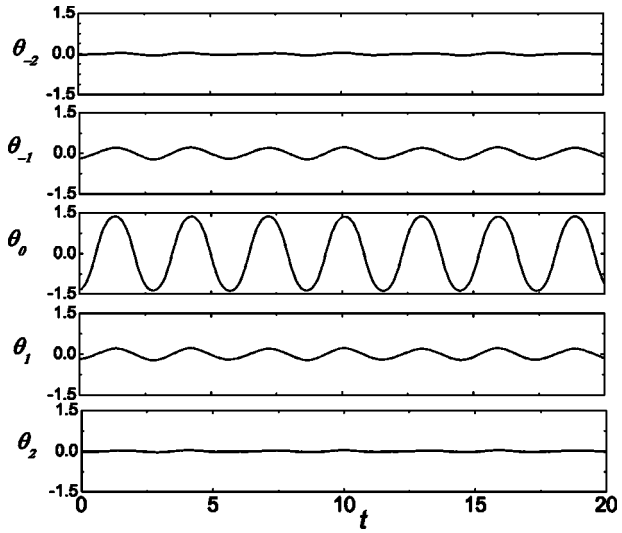

FIG. 6. ILM with all particles oscillating in one well of the on-site potential. The mode has amplitude $A_1 \approx 1.37$ and frequency $\omega \approx 2.15$, which is considerably lower than the bottom edge of the linear spectrum, $\omega_{\min} \approx 3.162$, with all higher harmonics lying above the upper edge, $\omega_{\max} \approx 3.847$. $J=1$, $\epsilon=0.2$, and $\lambda=5$.

$$\omega^2 = J[4(1+\epsilon)\sin^2(k/2) + 2\lambda], \quad (42)$$

with

$$\omega_{\min} = \sqrt{2J\lambda}, \quad \omega_{\max} = \sqrt{J[4(1+\epsilon) + 2\lambda]}. \quad (43)$$

When $\omega_{\max}/2 < \omega_{\min}$ [i.e., $\lambda > \frac{2}{3}(1+\epsilon)$], one can look for an ILM oscillating with frequency $\omega_{\max}/2 < \omega < \omega_{\min}$ so that all higher harmonics $l\omega$, with an integer $l>1$, lie above $\omega_{\max}$. In this situation the ILM would not interact with the lattice preserving its identity.

1. ILM with all particles in one potential well

As an example, we take $J=1$, $\epsilon=0.2$, and $\lambda=5$, with $\omega_{\min}=\sqrt{10} \approx 3.162$ and $\omega_{\max}=\sqrt{14.8} \approx 3.847$ so that the necessary condition of the existence of ILM, $\omega_{\max} < 2\omega_{\min}$, is fulfilled. A large-amplitude localized mode can be excited by choosing the initial deviation and/or initial velocity of a particle. As an example, we initialize the zeroth particle with $\theta_0(0)=1.5$, $\dot{\theta}_0(0)=0$ with zero initial conditions for other particles and, after some stabilization period, a steady oscillatory motion is observed (see Fig. 6). One can see that the ILM is highly localized. The mode has a frequency $\omega \approx 2.15$, which is considerably lower than the bottom edge of the linear spectrum $\omega_{\min}$ with all higher harmonics lying above the upper edge $\omega_{\max}$.

The ILM can be approximately expressed analytically assuming that

$$\theta_0(t) = A_1 \sin(\omega t) + A_3 \sin(3\omega t),$$

$$\theta_1(t) = \theta_{-1}(t) = B_1 \sin(\omega t),$$

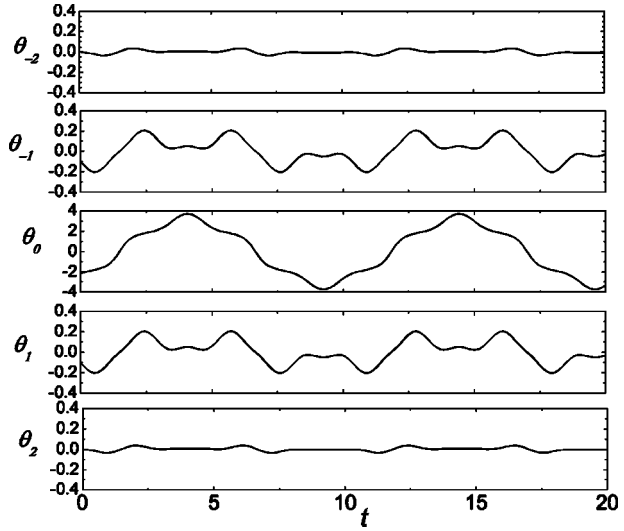

FIG. 7. Same as in Fig. 6 but for larger amplitude, $A_1 \approx 3.71$. The ILM has frequency $\omega \approx 0.607$ which is significantly lower than the bottom edge of the linear spectrum $\omega_{\min} \approx 3.162$. The mode radiates energy extremely slowly due to the interaction of higher harmonics with the linear spectrum. Note the difference in the ordinate scale for the middle panel. $J=1$, $\epsilon=0.2$, and $\lambda=5$.

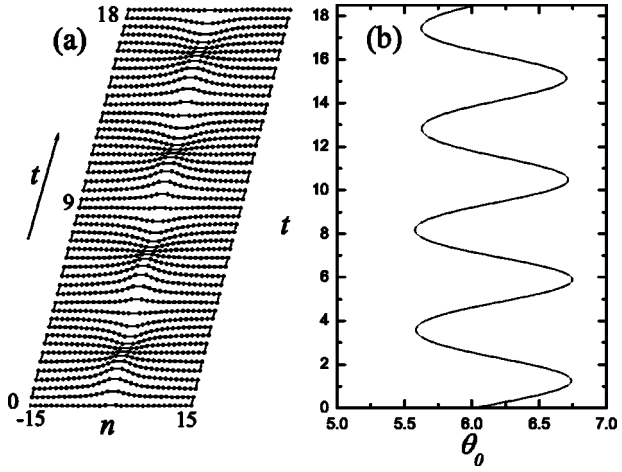

FIG. 8. ILM with one particle oscillating in a potential well different from that where other particles are located. (a) Plots θ vs n for different times showing the dynamics of particles (the zeroth particle is not shown here because its coordinate differs from coordinates of other particles significantly, by roughly 2π). (b) Dynamics of zeroth particle. The ILM is rather broad. The zeroth particle oscillates with the amplitude $A(\theta_0) \approx 0.6$ while its nearest neighbors have nearly the same amplitude, $A(\theta_{\pm 1}) \approx 0.52$, and the amplitudes decrease rather slowly with deviation from zeroth particle. $J=1$, $\epsilon=0.05$, and $\lambda=1$.

$$\theta_n(t) \equiv 0 \text{ for } |n| > 1, \tag{44}$$

with $A_3 \ll A_1$ and $B_1 \ll A_1$. Parameters of the approximate solution of Eq. (44) can be expressed in terms of the ILM amplitude A_1,

$$\omega^2 = J\left[2(1+\epsilon+\lambda) - \frac{1}{4}(1+4\lambda)A_1^2\right],$$

$$A_3 = \frac{(1+4\lambda)A_1^3}{12\left[9\frac{\omega^2}{J} - 2(1+\epsilon+\lambda)\right]},$$

$$B_1 = \frac{(1+\epsilon)A_1 - \frac{1}{8}A_1^3}{2(1+\epsilon+\lambda) - \frac{\omega^2}{J}}. \tag{45}$$

Let us analyze the obtained solution. First of all we note that the ILM frequency ω cannot be greater than $\omega_{\min}$, i.e., we can only look for a mode with frequency below $\omega_{\min}$ [see Eq. (43)], which is possible only for ILMs with sufficiently large amplitude,

$$A_1 > \sqrt{\frac{8(1+\epsilon)}{1+4\lambda}}. \tag{46}$$

For example, for $\epsilon=0.2$, and $\lambda=5$, one has $A_1 > 0.68$. We have confirmed numerically that, for this choice of parameters, our solution can be used for $A_1 \sim 1$.

For larger amplitudes the ILM is highly localized (see Fig. 7), but the solution [Eqs. (44) and (45)] becomes inaccurate because it takes into account only cubic anharmonicity. The ILM in Fig. 7 has amplitude $A_1 \approx 3.71$ and frequency $\omega \approx 0.607$, which is significantly lower the bottom edge of the linear spectrum $\omega_{\min} \approx 3.162$. The mode radiates energy extremely slowly due to the interaction of higher harmonics with the linear spectrum. Note the difference in the ordinate scale for the middle panel.

For small ILM amplitudes, approaching the allowed limit [Eq. (46)] the solution profile becomes wider and our assumption that it is localized on three particles becomes invalid. Estimation for the limiting amplitude [Eq. (46)] is also valid only for a highly localized ILM. In fact, it is possible to excite an ILM with a very small amplitude, but the width of such ILM increases considerably and its frequency approaches $\omega_{\min}$ from below. The smooth transformation of the ILM from a highly localized (as the amplitude decreases) into a very broad one is not surprising because for smooth solutions, $(\theta_{n+1}-\theta_n) \ll 1$, one has $\sin(\theta_{n+1}-\theta_n) \approx (\theta_{n+1}-\theta_n)$ and the SLL with the on-site potential [Eq. (41)] can be approximated by the well-known continuum sine-Gordon equation. The ILM is, then, nothing but the analog of breather solution to the sine-Gordon equation. Using the Lorentz invariance of the sine-Gordon equation one can create a moving small-amplitude breather.

We also note that, when $\epsilon \gg 1$ and $\lambda \gg 1$, the first two terms on the right-hand side of Eq. (41) can be neglected. In this situation, when ϵ and λ are of the same order of magnitude, our solution [Eqs. (44) and (45)] describes a highly localized ILM in the Frenkel-Kontorova model.[25]

2. ILM with one particle in a different potential well

The SLL lattice with on-site potential supports localized modes of another type, when one particle is trapped in a

potential well different from the well occupied by the other particles. To demonstrate this mode, we take $J=1$, $\epsilon=0.05$, and $\lambda=1$, with $\omega_{\min}=\sqrt{2}\approx 1.414$, and $\omega_{\max}=\sqrt{6.2}\approx 2.490$ so that the necessary condition $\omega_{\max}<2\omega_{\min}$ is fulfilled. Setting $\theta_0(0)=2.9$, $\dot{\theta}_0(0)=0$ with zero initial conditions for other particles, after some time a steady oscillatory motion presented in Fig. 8 was observed. The zeroth particle was found to oscillate with $\omega\approx 1.35$, which is below the linear vibration band, but all higher harmonics are above the band. One can see that the ILM is not highly localized. The zeroth particle oscillates with the amplitude $A(\theta_0)\approx 0.6$ near the coordinate shifted by roughly 2π with respect to the neutral position of all other particles [shown in Fig. 8(b)]. Its nearest neighbors oscillate with nearly the same amplitude, $A(\theta_{\pm 1})\approx 0.52$, and the amplitudes decrease rather slowly with deviation from the zeroth particle [see Fig. 8(a)].

VI. CONCLUDING REMARKS

In this paper, we have outlined a general scheme to apply geometrical constraints to a simplified version of the 3D harmonic lattice with or without an on-site potential to obtain nonlinear dynamical lattice equations. Depending on the type of the constraints, we arrive at various nonlinear equations, being interested in the coherent structures that arise in them.

We then studied, more specifically, a helical constraint by which the original 3D harmonic lattice was shown to reduce to 1D sine-plus-linear lattice equations or helical lattice equations. This formulation revealed several interesting features:

(i) It provides us with a systematic derivation of the sine-lattice equations, which were derived heuristically in earlier works.

(ii) Physically, applying the helical constraint amounts to transforming the original harmonic lattices (possessing the hard potential) to a nonlinear dynamical lattice that supports resonant and multikink modes. Seeking other kinds of nonlinear modes will be an interesting topic for future study.

(iii) The method developed here may be relevant to the study of nonlinear excitations in biomolecules with helical structure, such as DNA and proteins. There are several areas of condensed-matter physics where the existence of a complex energy landscape with a number of local minima in the potential function is presumed to play a crucial role in determining their properties. Such examples can, for instance, be found in the study of glasses and proteins. Application of the techniques employed here to these problems would be another topic warranting further investigation.

(iv) Finally, another relevant generalization would be to consider geometric constraints different from the helical one and to derive and study the ensuing (reduced) dynamical models.

These topics are currently under study and will be reported elsewhere.

This work was partially financially supported by NSF-DMS-0204585, NSF-CAREER, and the Eppley Foundation for Research (PGK). Work at Los Alamos is supported by the US DoE.

[1] S. Takeno, Prog. Theor. Phys. **75**, 1 (1986); S. Takeno, K. Kisoda, and A. Sievers, Prog. Theor. Phys. Suppl. **94**, 242 (1988).
[2] A. J. Sievers and S. Takeno, Phys. Rev. Lett. **61**, 970 (1988).
[3] For recent reviews, see for example, S. Flach and C. R. Willis, Phys. Rep. **295**, 181 (1998); D. Hennig and G. Tsironis, *ibid.* **307**, 333 (1999); P. G. Kevrekidis, K. O. Rasmussen, and A. R. Bishop, Int. J. Mod. Phys. B **15** (2001) 2833–2900; J. Ch. Eilbeck and M. Johansson, in *Localization and Energy Transfer in Nonlinear Systems*, edited by L. Vazquez, R. S. MacKay and M. P. Zorzano (World Scientific, Singapore, 2003), p. 44.
[4] U. T. Schwarz, L. Q. English, and A. J. Sievers, Phys. Rev. Lett. **83**, 223 (1999).
[5] N. K. Voulgarakis, G. Kalosakas, A. R. Bishop, and G. P. Tsironis, Phys. Rev. B **64**, 020301(R) (2001) and references cited therein.
[6] E. Trías, J. J. Mazo, and T. P. Orlando, Phys. Rev. Lett. **84**, 741 (2000); P. Binder, D. Abraimov, A. V. Ustinov, S. Flach, and Y. Zolotaryuk, *ibid.* **84**, 745 (2000).
[7] For a very recent review on the latest developments, see, e.g., D. K. Campbell, S. Flach, and Y. Kivshar, Phys. Today **57**, 43 (2004).
[8] See, e.g., P. G. Kevrekidis, B. A. Malomed, and A. R. Bishop, Phys. Rev. E **66**, 046621 (2002) and references cited therein.
[9] S. Yomosa, Phys. Rev. A **27**, 2120 (1983); **30**, 474 (1984).
[10] S. Homma and S. Takeno, Prog. Theor. Phys. **72**, 679 (1984).
[11] S. Takeno and S. Homma, J. Phys. Soc. Jpn. **65**, 2547 (1986).
[12] S. Takeno and M. Peyrard, Physica D **92**, 142 (1996); Phys. Rev. E **55**, 1922 (1997).
[13] K. W. Wojciechowski, K. V. Tretiakov, and M. Kowalik, Phys. Rev. E **67**, 036121 (2003).
[14] J. Cuevas J. F. R. Archilla, Yu. B. Gaididei, and F. R. Romero, Physica D **163**, 106 (2002).
[15] Y. B. Gaididei, S. F. Mingaleev, and P. L. Christiansen, Phys. Rev. E **62**, R53 (2000).
[16] S. A. Wells, M. T. Dove, M. G. Tucker, and K. Trachenko, J. Phys.: Condens. Matter **14**, 4645 (2002).
[17] M. Vallade, B. Berge, and G. Dolino, J. Phys. I **2**, 1481 (1992).
[18] S. V. Dmitriev, D. A. Semagin, T. Shigenari, K. Abe, M. Nagamine, and T. A. Aslanyan, Phys. Rev. B **68**, 052101 (2003); D. A. Semagin, S. V. Dmitriev, K. Abe, and T. Shigenari, Russ. J. Phys. Chem. **77**, S30 (2003). S. V. Dmitriev, A. A. Vasiliev, and N. Yoshikawa, in *Recent Research Developments in Physics*, edited by S. G. Pandalai (Transworld Research Network, Kerala, India, 2003), Vol. 4, Part I, pp. 267–286.
[19] H. Kimizuka, H. Kaburaki, and Y. Kogure Phys. Rev. Lett. **84**, 5548 (2000).
[20] M. B. Smirnov and A. P. Mirgorodsky, Phys. Rev. Lett. **78**, 2413 (1997).
[21] N. R. Keskar and J. R. Chelikowsky, Phys. Rev. B **48**, 16 227

(1993).
[22] A. Alderson and K. E. Evans, Phys. Rev. Lett. **89**, 225503 (2002).
[23] M. B. Smirnov, Phys. Rev. B **59**, 4036 (1999).
[24] P. G. Kevrekidis, S. V. Dmitriev, S. Takeno, A. R. Bishop, and E. C. Aifantis, Phys. Rev. E (to be published).
[25] O. M. Braun, and Y. S. Kivshar, *The Frenkel-Kontorova Model: Concepts, Methods, and Applications*,(Springer-Verlag, Berlin, 2004).
[26] P. G. Kevrekidis and V. V. Konotop, Phys. Rev. E **65**, 066614 (2002); P. G. Kevrekidis, V. V. Konotop, and S. Takeno, Phys. Lett. A **299**, 166 (2002).